Effects of ultrasonic melt processing on microstructure, mechanical properties and electrical conductivity of hypereutectic Al-Si, Al-Fe and Al-Ni alloys with Zr additions

Suwaree Chankitmunkong[1, a*], Dmitry G. Eskin[2, 3, b], and Chaowalit Limmaneevichitr[4, c]
[1]Department of Industrial Engineering, Faculty of Engineering, King Mongkut's Institute of Technology Ladkrabang, Chalongkrung Road, Ladkrabang, Bangkok 10520 Thailand
[2]Brunel University London, BCAST, Uxbridge, Middlesex UB8 3PH, United Kingdom
[3]Tomsk State University, Tomsk 634050, Russian Federation
[4]Department of Production Engineering, Faculty of Engineering, King Mongkut's University of Technology Thonburi, 126 Pracha-Utid Rd., Bangmod, Tungkhru, Bangkok, 10140 Thailand
[a*]suwaree.03@mail.kmutt.ac.th, [b]dmitry.eskin@brunel.ac.uk, [c]chaowalit.lim@mail.kmutt.ac.th
Corresponding Author[*] S. Chankitmunkong, Email: suwaree.03@mail.kmutt.ac.th

Abstract

Ultrasonic melt processing (USP) technique was used to study the effect of Zr addition on the structure refinement and mechanical properties of hypereutectic binary alloy in three different alloys (Al-Si, Al-Fe and Al-Ni) as potential alternatives to the Al-Si eutectic system especially for high-temperature applications. Mechanical properties of these alloys were controlled through both structure refinement by USP and also Al_3Zr nano-precipitation hardening. Significant refinement of primary intermetallics was achieved under USP during the Al_3Zr formation in solidification process. The residual Zr in the aluminium solid solution enabled precipitation hardening at 450 °C. As a result, the tensile properties, especially ductility, were considerably improved at room and elevated temepratures. The mechanical properties were analyzed with respect to the volume fraction of intermetallic phases. Electrical conductivity was measured to better explore their potential applications. The effects of alloying elements and structure changes on the mechanical behaviour and electrical conductivity were discussed.

Keywords: Al-Si alloy, Al-Fe alloy, Al-Ni alloy, mechanical properties, ultrasonic melt processing, Mechanical properties

Introduction

Hypereutectic aluminum alloys are extensively used in automotive industry due to their excellent casting characteristic, high strength to weight ratio, and low prices [1, 2]. However, it was reported that high Si content in Al-Si alloys affected the mechanical properties and might lead to loss in electrical conductivity [3]. Most recently, new types of hypereutectic Al-Ni and Al-Fe alloys attract considerable interest as candidate materials for automotive and electrical applications [4].

Normally, aluminum alloys used for electrical conductivity applications are not grain refined because the addition of commercial grain refiners such as Al-Ti-B can adversely affect the electrical conductivity by adding unstable impurities of AlB_2 and AlB_{12} that cannot be dissolved into the melt [5]. It is well known that transition metals such as Ti and Zr, that are used for grain control, may also lead to the decrease in electrical conductivity [6]. However, the non-grain refined microstructure may result in fracture and other defects in a wire drawing process [7].

In previous works, the mechanical properties of hypereutectic alloys were studied and reported depending on the formation of hard primary intermetallics, including the volume fraction

and size of intermetallics. It is clear that there is a necessity to refine the brittle intermetallics in hypereutectic alloy to achieve the required properties.

One of the effective methods to refine primary intermetallics is ultrasonic melt processing (USP) through the main mechanism of nucleation and fragmentation, which results in the refinement of both grains and intermetallics thus improving the strength and ductility of the materials [8]. Thus, the necessity of adding grain refiner can be reduced. Moreover, the combined effect of USP and addition of Zr to aluminum alloys was reported to be effective in structure refinement [9], which included enhanced nucleation of the primary Al_3Zr phase on activated oxides [10] followed by fragmentation of these primary intermetallics caused by cavitation [11]. These refined particles act as solidification sites for the Al solid solution and intermetallics. It is very interesting to define the optimum balance between the USP-refined microstructure for deformation process with the minimum decrease of electrical conductivity, and also high mechanical properties for high-temperature applications.

Therefore, this work aims to investigate the effects of USP on microstructure of hypereutectic alloys and mechanical properties at elevated temperature, and also on the electrical conductivity to assess the feasibility of broader applications.

Experimental procedure

The three experimental hypereutectic allloys, i.e. Al-16Si-0.3Zr, Al-4Fe-0.3Ze and Al-8Ni-0.3Zr (all alloys are named in wt% unless otherwise stated), were prepared using high-pure Al (99.99 %), pure cystalline Si, Al-17.5%Ni, Al-10% Ni and Al-5% Zr master alloys. The alloys were melted in a silicon carbide crucible using an induction furnace and then poured at temperatures of 690 °C, 710 °C and 730 °C for Al-16Si-0.3Zr, Al-8Ni-0.3Zr and Al-4Fe-0.3Zr, respectively. Ultrasonic melt processing was performed by dipping a pre-heated (500 °C) niobium sonotrode 20 mm in diameter into the melt in the crucible by approximately 5 mm below the melt surface prior to casting. A 20-kHz air-cooled piezoelectric transducer was used. The USP was applied in the molten metals of experimental alloys in the temperature range of 750 to 690 °C for Al-16Si-0.3Zr alloy, 740 to 710 °C for Al-8Ni-0.3Zr alloy and 780 to 730 °C for Al-4Fe-0.3Zr alloy. The selected temperatures were based on solidification ranges of primary phase in each experiemental alloy. The cast specimens were prepared according to standard grinding and polishing procedure to observe the microstructure. Image analysis technique (Image J) was used to analyse the area fraction and average size of intermetallics for each alloy system. The presence of Al_3Zr intermetallic was characterized with a ZEISS Supra 35 SEM. The castings were machined to round tensile specimens following the ASTM-B557M standard (6 mm diameter, 30 mm gauge length) and treated at 450 °C for 30 h to obtain the saturated hardness values of the alloys through the precipitation of Al_3Zr (L_{12}) [12, 13] before performing tensile tests. High-temperature tensile tests were performed in a universal testing machine (Instron model 5969) at a strain rate of 0.05/s. The values of ultimate tensile strength (UTS), yield strength (YS) and elongation (%El) were obtained from 3 specimens with standard deviation calculation. The fracture surfaces were observed in an optical microscope through the cross section along the tension direction to better understand the failure mechanism. Electrical conductivity measurements were performed using a Sigmatest 2.069 eddy current conductivity tester (Forester Instrument). For each sample, ten measurements were conducted at 120 kHz.

Results and Discussion

Intermetallics refinement of hypereutectic alloys

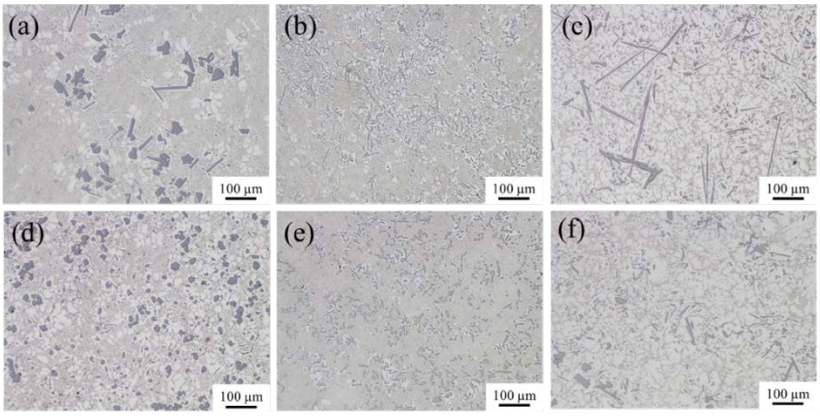

Figure 1 Microstructure of experimental alloys (a-c) without USP, and (d-f) with USP; (a, d) Al-16Si-0.3Zr, (b, e) Al-8Ni-0.3Zr and (c, f) Al-4Fe-0.3Zr.

The main microstructure features of the hypereutectic alloys are primary intermetallics and eutectic grains. **Figure 1** shows microstructures of experimental alloys that were treated with USP and without USP. The results showed that hypereutectic Al-16Si, Al-4Fe and Al-8Ni with 0.3 wt% Zr addition formed large primary intermetallics of Si, Fe and Ni as can be seen in **Fig.1(a-c)**, respectively. However, these intermetallics were refined after ultrasonic melt processing during solidification ranges of each alloys as shown in **Fig. 1(d-f).** This can be explained through the structure refinement mechanisms reported elsewhere, i.e. nucleation [14] and fragmentation of intermetallics [9-11].

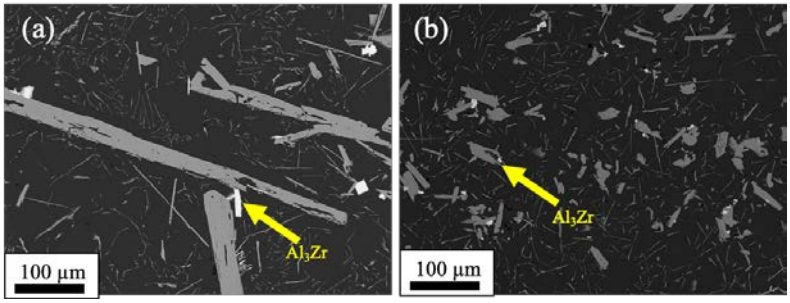

Figure 2 SEM images showing the interaction between primary Al_3Zr crystals and other phases in hypereutectic alloys of (a) Al-4Fe-0.3Zr without USP, (b) Al-4Fe-0.3Zr with USP treatment.

Figure 2 shows the location of small primary Al_3Zr crystals in the overall microstructure. The results confirm that the Al_3Zr particles were refined and distributed along with the refined Fe containing intermetallics (Al_3Fe) in the alloy that was treated by USP. These Al_3Zr particles are either located in the center of eutectic colonies or connected to Al_3Fe. This illustrated the possibility of a refining mechanism by the Al_3Zr phase nucleating primary Al_3Fe and being also substrates for the eutectic colonies, therefore, refining both intermetallics and eutectic grains. This mechanism is quite similar to the previously suggested one for Al grains [10, 11].

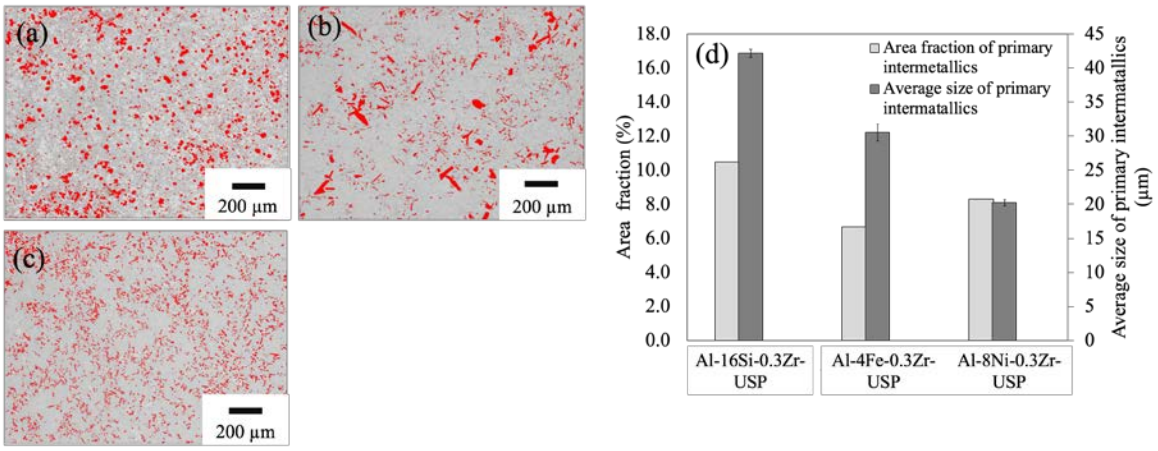

Figure 3 Image analysis of the area fraction of primary intermetallics of the different hypereutectic alloys that were treated by USP; (a) Al-16Si-0.3Zr, (b) Al-4Fe-0.3Zr, (c) Al-8Ni-0.3Zr, and (d) the qualitative results of area fraction (%) and average size of primary intermetallics.

Figure 3 gives the amount of the area fraction and the average size of primary intermetallics in three alloys that were refined by USP as measured by image analysis (the average size and area fraction). The Al-8Ni-0.3Zr alloys demonstrated more uniform distribution of small intermetallics in the Al matrix, while the Al-16Si-0.3Zr alloy had the largest area fraction and average size of the Si phase.

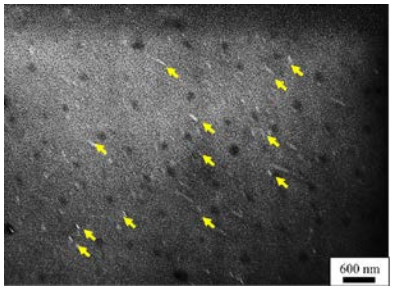

Figure 4 A SEM image of Al_3Zr nano-precipitates in the Al-4Fe-0·3Zr alloy with USP after exposure at 450 °C for 30 h.

The formation of metastable Al_3Zr precipitates in a hypereutectic Al-4Fe-0.3Zr alloy after high-temperature exposure was examined by SEM and the results showed the presence and uniform distribution of Al_3Zr nano-precipitates in Al-grains as pointed by yellow arrows in **Fig. 4.** The result is consistent with previous work that investigated the precipitation of Al_3Zr in the Al-matrix [15]. It is also expected to have similar precipitation in other hypereutectic Al-16Si-0.3Zr and Al-8Ni-0.3Zr alloys that have the same amount of Zr addition (0.3%).

Strength and ductility of hypereutectic alloys upon USP

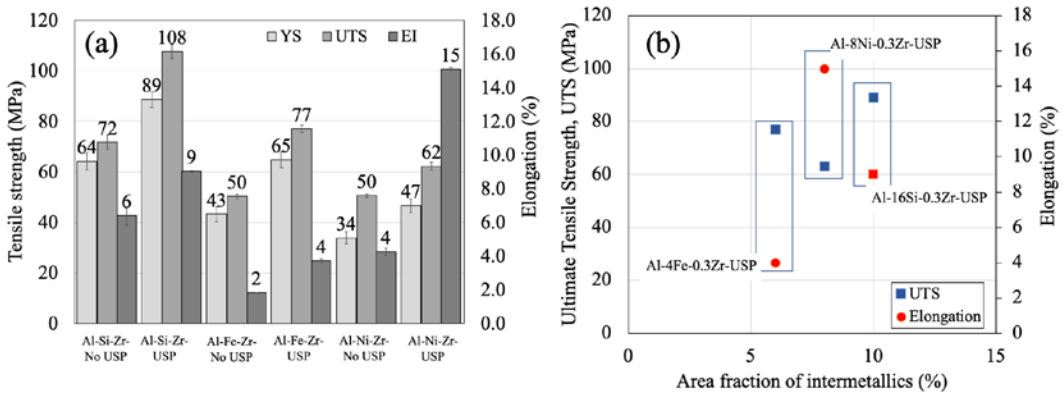

Figure 5 The average value of mechanical properties (UTS, YS, El) at 300 °C of the aged specimens (a), and (b) the correlation of the mechanical properties to the area fraction of hard primary intermetallics.

In general, the tensile strength of aged hypereutectic alloys at a high temperature of 300 °C depends on the presence of primary intermetallics that are formed in the microstructure. The average values of tensile properties including ultimate tensile strength (UTS), yield strength (YS) and percentage elongation (%El) of the experimental alloys at high temperature of 300 °C are shown in **Fig. 5 (a)**. The results showed that the application of USP improves strength and ductility in all experimental alloys.

Note that among the hypereutectic alloys, Al-16Si-0.3Zr has the highest UTS and YS after USP, while Al-8Ni-0.3Zr demonstrated the highest ductility. To better analyze the relationship of microstructure and mechanical properties, the comparison of the amount of hard particles in each hypereutectic alloys with the mechanical properties were correlated and given in **Fig. 5 (b).** The results showed that the highest UTS in Al-16Si-0.3Zr came along with higher area fraction of hard particles, which also led to the reduced elongation. While the optimum combination of UTS and elongation can be found in the hypereutectic Al-8Ni-Zr alloy, which may be because of the beneficial ratio of the lower area fraction of hard particles and the smaller size of intermetallics as shown in **Fig.3(c, d).**

The presence of Zr in the solid solution after solidification and its precipitation at 450 °C as shown in **Fig. 4** may additionally contribute to the hardening of all studies alloys as demonstrated elsewhere [8]. This hardening effect will be of course preserved at 300 °C.

Fractographic observations

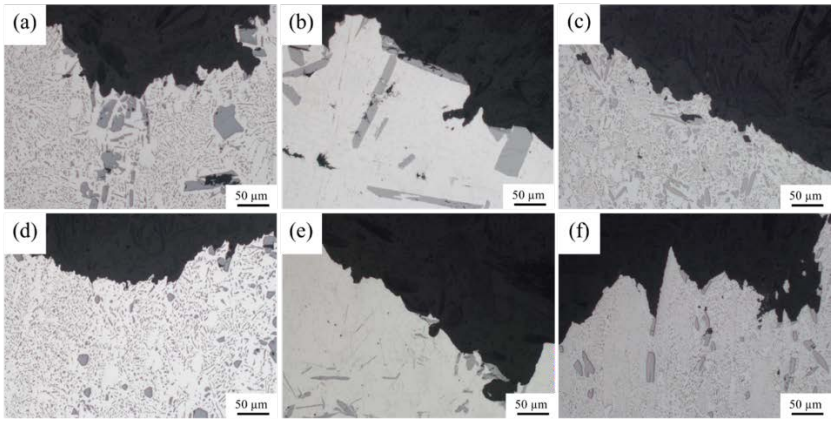

Figure 6 Fracture surface of annealed samples after tensile testing at 300 ℃ of different experimental alloys that were cast without USP (a-c), and the samples that were cast with USP (d-f); (a, d) Al-16Si-0.3Zr, (b, e) Al-4Fe-0.3Zr, (c, f) Al-8Ni-0.3Zr.

To better understand fracture behavior and fracture mode of hypereutectic Al-16Si, Al-4Fe and Al-8Ni alloys with 0.3% Zr addition, fractured tensile test specimens were investigated as shown in **Fig. 6.** It is clear that the cracks on the fracture surface initiated at the large intermetallics of primary Si, Al_3Fe and Al_3Ni intermetallics and propagated along the interface between the intermetallic and eutectic phases. In USP sample, however, the propagation of the crack tended to go through the solid solution/eutectic matrix with much less stress concentration on the refined intermetallics, which explains the simultaneous improvement of tensile strength and ductility in USP treated alloys.

Electrical conductivity

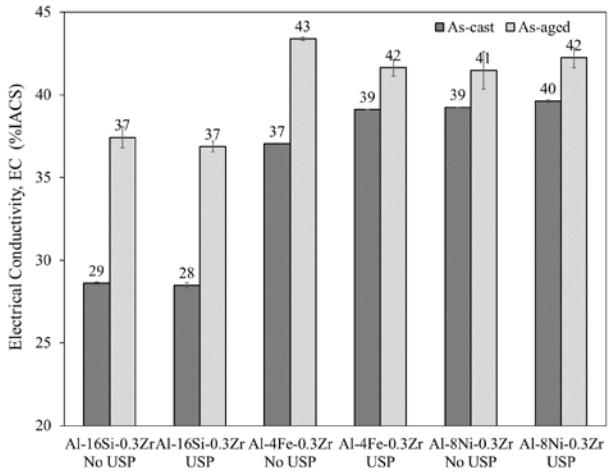

Figure 7 Electrical conductivity of three hypereutectic alloys of Al-16Si, Al-4Fe and Al-8Ni with 0.3 wt% Zr addition

For potential electric applications, three types of hypereutectic alloys with Zr addition that were cast with and without USP were investigated for the electrical conductivity.

Figure 7 illustrates the electrical conductivity of as-cast and annealed samples of experimental alloys that were treated in different conditions. The results show that among all of the tested hypereutectic alloys, the electrical conductivity of the Al-4Fe-0.3Zr and Al-8Ni-0.3Zr alloys were consistently higher than the Al-16Si-0.3Zr alloy in both as-cast and aged conditions. This is due to the fact that Fe and Ni elements have less detrimental effect on the conductivity of aluminum due to their lower solid solubility [16, 17]. Both Al-4Fe-0.3Zr and Al-8Ni-0.3Zr alloys have their lowest measured conductivity (37-40 % IACS) substantially higher than those of conventional alloys (28 % IACS) [3]. The results also showed that the electrical conductivity increased when the alloys were further treated in annealed at 450 °C. This is the result of Zr precipitation from the aluminum solid solution so that almost pure Al remains to assure good electrical conductivity. At the same time, USP does not provide extra benefits for the electrical conductivity. Its benefits are in the grain and intermetallics refinement with the overall improvement of mechanical properties without reducing the electrical conductivity.

Conclusion

- The structure refinement in hypereutectic Al-Si, Al–Fe and Al–Ni alloys with addition of Zr can be achieved by ultrasonic melt processing in the range of primary intermetallic solidification.
- The Al-4Fe-0.3Zr and Al-8Ni-0.3Zr alloys have higher electrical conductivity as compared to the hypereutectic Al-16Si-0.3Zr alloy.
- The ultrasonic melt processing can be used to achieve structure refinement, improvement of mechanical properties (both strength and ductility) while retaining high electrical conductivity.
- The tensile properties of hypereutectic alloys are related to the area fraction and size of refined primary intermetallics.

Acknowledgements

The authors gratefully acknowledge Faculty of Engineering at KMUTT for its financial support from the Strong Research Initiative 2020 and the financial support from EPSRC (UK) under project UltraMelt2 (EP/R011095/1).

References

[1] N. Raghukiran, R. Kumar, Effect of scandium addition on the microstructure, mechanical and wear properties of the spray formed hypereutectic aluminum–silicon alloys, Mater. Sci. Eng., A 641 (2015) 138-147.

[2] Z. Cai, R. Wang, C. Zhang, C. Peng, L. Xie, L. Wang, Characterization of Rapidly Solidified Al-27 Si Hypereutectic Alloy: Effect of Solidification Condition, J. Mater. Eng. Perform. 24(3) (2015) 1226-1236.

[3] M. Mulazimoglu, R. Drew, J. Gruzleski, The electrical conductivity of cast Al− Si alloys in the range 2 to 12.6 wt pct silicon, Metall. Trans. A 20(3) (1989) 383-389.

[4] F. Průša, D. Vojtěch, A. Michalcová, I. Marek, Mechanical properties and thermal stability of Al–Fe–Ni alloys prepared by centrifugal atomisation and hot extrusion, Mater. Sci. Eng., A 603 (2014) 141-149.

[5] A. Khaliq, M.A. Rhamdhani, G.A. Brooks, J. Grandfield, Removal of Vanadium from Molten Aluminum—Part III. Analysis of Industrial Boron Treatment Practice, Metallurgical and Materials Transactions B 45(2) (2014) 784-794.
[6] A. Khaliq, M. Rhamdhani, G.A. Brooks, J. Grandfield, Thermodynamic analysis of Ti, Zr, V and Cr impurities in aluminum melt, Light Metals 2011, Springer2011, pp. 751-756.
[7] L. Metlov, A. Zavdoveev, E. Pashinska, Merging of the grains during wire drawing, arXiv preprint arXiv:1508.02181 (2015).
[8] G.I. Eskin, D.G. Eskin, Ultrasonic treatment of light alloy melts, CRC Press2015.
[9] S. Chankitmunkong, D.G. Eskin, C. Limmaneevichitr, Structure refinement, mechanical properties and feasibility of deformation of hypereutectic Al–Fe–Zr and Al–Ni–Zr alloys subjected to ultrasonic melt processing, Mater. Sci. Eng., A (2020) 139567.
[10] T.V. Atamanenko, D.G. Eskin, M. Sluiter, L. Katgerman, On the mechanism of grain refinement in Al–Zr–Ti alloys, J. Alloys Compd. 509(1) (2011) 57-60.
[11] T. Atamanenko, D. Eskin, L. Zhang, L. Katgerman, Criteria of grain refinement induced by ultrasonic melt treatment of aluminum alloys containing Zr and Ti, Metallurgical and Materials Transactions A 41(8) (2010) 2056-2066.
[12] S. Chankitmunkong, D.G. Eskin, C. Limmaneevichitr, Microstructure evolution in an Al-Si piston alloy under ultrasonic melt processing, IOP Conference Series: Materials Science and Engineering, IOP Publishing, 2019, p. 012060.
[13] K.E. Knipling, R.A. Karnesky, C.P. Lee, D.C. Dunand, D.N. Seidman, Precipitation evolution in Al–0.1 Sc, Al–0.1 Zr and Al–0.1 Sc–0.1 Zr (at.%) alloys during isochronal aging, Acta Mater. 58(15) (2010) 5184-5195.
[14] F. Wang, D. Eskin, J. Mi, T. Connolley, J. Lindsay, M. Mounib, A refining mechanism of primary Al 3 Ti intermetallic particles by ultrasonic treatment in the liquid state, Acta Mater. 116 (2016) 354-363.
[15] S.Y. Jiang, R.H. Wang, Manipulating nanostructure to simultaneously improve the electrical conductivity and strength in microalloyed Al-Zr conductors, Scientific Reports 8(1) (2018) 6202.
[16] M. Jabłoński, T. Knych, B. Smyrak, New aluminium alloys for electrical wires of fine diameter for automotive industry, Archives of Metallurgy and Materials 54(3) (2009) 672-676.
[17] L.F. Mondolfo, Aluminum Alloys: Structure and Properties, Butterworths, Boston, 1976.